Langmuir−Blodgett Patterning of Phospholipid Microstripes: Effect of the Second Component

Xiaodong Chen,[†] Nan Lu,[‡] Hui Zhang,[‡] Michael Hirtz,[†] Lixin Wu,[‡] Harald Fuchs,[†] and Lifeng Chi*[,†]

Physikalisches Institut and Center for Nanotechnology (CeNTech), Westfälische Wilhelms-Universität, D-48149 Münster, Germany, and Key Laboratory for Supramolecular Structure and Materials of Ministry of Education, Jilin University, 130023, Changchun, People's Republic of China

Received: January 13, 2006; In Final Form: March 6, 2006

We systematically describe the striped pattern formation of the mixed monolayers of 1,2-di(2,4-octadecadienoyl)-*sn*-glycero-3-phosphocholine (DOEPC) and L-α-dipalmitoylphosphatidylcholine (DPPC) from the liquid expanded (LE) phase onto a mica surface by Langmuir−Blodgett (LB) transfer. The addition of the second component, DOEPC, strongly affects the formation of DPPC stripe patterns. When the molar ratio of DPPC and DOEPC is 1:0.1, the horizontal stripes dominate, while in the case of pure DPPC monolayer, there are three kinds of patterns: horizontal stripes, grids, and vertical stripes. The width and periodicity of stripes formed from the mixed monolayers are ca. 4−5 times smaller than those formed from pure DPPC patterns at the same transfer conditions, while the widths of channels are similar. A phase shift of substrate-mediated microphase separation in the two-component system during LB transfer is considered to be the mechanism for the influence of the second component on the formation of DPPC stripe patterns.

Introduction

Self-assembly and self-organization provide interesting routes toward the fabrication of patterned structures (from a few nanometers to micrometers in feature size) via a bottom-up approach.[1] The self-assembly and self-organization processes and the properties of the surface patterns (shape, size, function, etc.) can be controlled by tailoring the properties of building blocks. Two typical examples are block copolymer lithography,[2] where structures depend on the preparation conditions as well as the chemical properties of participating polymer fragments, and nanosphere lithography,[3] where the lateral dimensions can be controlled by varying the diameter of spherical colloids. Recently, it has been realized that the well-known Langmuir−Blodgett (LB) technique is another efficient way toward the fabrication of laterally patterned structures on solid supports that are chemically or physically differentiated on the micron or submicron scale, termed LB patterning here.

Normally, laterally structured LB monolayers are generated by the deposition of regular two-dimensional (2D) domains formed at the air−water interface onto solid substrates. The shape of domains at the air−water interface can be extensively controlled by subphase conditions (e.g., composition and temperature), external electrical fields, molecular chirality, and the molecular composition of the monolayer.[4−6] The domains of shapes depend on two competing effects: interfacial line tension between the two lipid phases that favors circular domains, and repulsive dipole forces between the lipid molecules that favor elongated shapes.[4,5] Alternatively, the LB transfer process itself can be used to induce phase transitions and pattern formation near the three phase contact line from a homogeneous Langmuir monolayer, which was directly observed by fluorescence microscopy.[7,8] Schwartz et al. observed dendritic patterns when fatty acids deposited from the liquid expanded (LE) phase undergo a substrate-induced phase transition on substrates to the liquid condensed (LC) phase.[9,10] Previously, we described the formation of L-α-dipalmitoylphosphatidylcholine (DPPC) stripe patterns by the LB transfer of the DPPC monolayer at the surface pressures below the LE−LC phase transition pressure.[11,12] The pattern formation was attributed to substrate-mediated first-order phase transition of DPPC, being a typical example of "self-organization", and meniscus oscillation during LB transfer. Just as its name implies, the molecule−substrate interaction plays a very important role in the condensation process. Recently, Badia et al.[13,14] generated the pattern with parallel stripes by the LB transfer of a mixed phospholipid (DPPC and DLPC (L-α-dilauroylphosphatidylcholine)) monolayer from the air−water interface onto a mica substrate; however, they suggested that the stripe formation in the mixed films is due to a cyclical condensed-phase nucleation and depletion process that is coupled to dynamic wetting instabilities,[13] not due to substrate-mediated condensation.[9−12] The difference is that Badia et al. transferred the mixed monolayer at high surface pressure, where DPPC is already in the LC state, while we transfer the monolayer below the phase transition point where DPPC is in the LE state.[11,12] Similar to the case of Badia et al., Purrucker et al.[15] reported a stripe micropattern on a solid substrate from a lipid/lipopolymer mixed monolayer by the LB transfer; however, the stripes are aligned perpendicular to the meniscus, which has also been observed in the case of pure DPPC.[16,17] Analogous stripe patterns (parallel to the meniscus) of fatty acid monolayers on mica surface, depending on the pH, were found by Vollhardt et al.[18,19] In this case, there is no phase transition (as the floating monolayer is already in a condensed phase) taking place during the LB transfer but rather a transition

* Corresponding author. Phone: +49-251-83-33651. Fax: +49-251-83-33602. E-mail: chi@uni-muenster.de.
[†] Westfälische Wilhelms-Universität.
[‡] Jilin University.

10.1021/jp0602530 CCC: $30.25
Published on Web 03/31/2006

from arachidic acid to cadmium arachidate at pH ~5.7 in the presence of cadmium salt.

LB patterning has shown promising application in numerous areas. The generated DPPC stripe patterns show a selective, anisotropic wetting property,[20] which can be used as a template to guide the self-assembly of chemical functionalities, such as nanoparticles,[12,21] proteins,[22] and transmembrane cell receptors.[15] The obtained DPPC stripe patterns do not change after the obtained samples are kept in ambitious conditions for at least 6 months. Furthermore, combined with template-directed self-assembly, we successfully obtained chemically patterned surfaces,[23] which are stable in water and organic solvents. For instance, the chemical stripe patterns can be used as templates to assist in electrodeposition of submicrometer-wide wires in a regular array,[24] as well as allowing pattern transfer by chemical etching.[16] There are also applications in directing the growth of cells, such as osteoblasts, which show significant anisotropic behavior on topographical patterns fabricated by means of the LB stripe patterns.[16,25] In addition, luminescent stripe patterns with submicron-scale lateral dimensions over large areas can be obtained by simply transferring dye/DPPC mixed monolayers onto a solid substrate at suitable conditions.[26]

The ability to control stripe patterns is essential to their application in all of the above descriptions. Mixed monolayers have brought more and more interest in monolayer research due to the wider variety of properties of a multicomponent systems than those of pure monolayers.[4,27] For a mixed monolayer, the miscibility of various components is important in regard to the phase behavior and the stability of the monolayer. Similarly, the second component should play a very important role in the process of substrate-mediated condensation during LB deposition. In the present paper, we systematically study the effect of the second component on the formation of DPPC stripe patterns on the solid substrate by LB hydrophilic deposition. There are many works on the phase behavior of binary lipids at the air−water interface,[5,28,29] where phase separation is a normal phenomenon for the phospholipids with the same headgroup but different hydrocarbon chain lengths or degrees of saturation.[30] Therefore, here we select 1,2-di(2,4-octadecadienoyl)-*sn*-glycero-3-phosphocholine (DOEPC) as the second component, since DOEPC forms a fully LE phase at the air−water interface and does not show the behavior of substrate-mediated condensation during LB transfer under the conditions where DPPC forms stripes. As a control, we first describe the DPPC stripe pattern formation from the pure DPPC monolayer depending on the transfer conditions (surface pressure and velocity). Then, we investigate the effect of DOEPC on the formation of DPPC stripe in detail (different transfer conditions and molar ratio of DPPC and DOEPC). Finally, we show that other kinds of lipid components can also be used to affect the formation of DPPC stripe patterns.

Experimental Section

Materials. L-α-Dipalmitoylphosphatidylcholine (DPPC) was obtained as a powder from Fluka and used without further purification (chemical purity >99%). 1,2-Dipalmitoleoyl-*sn*-glycero-3-phosphocholine (DPOPC) was purchased from Avanti Polar Lipids (Alabaster, AL). 1,2-Di(2,4-octadecadienoyl)-*sn*-glycero-3-phosphocholine (DOEPC) was synthesized according to ref 31. Details of the synthesis are provided in the Supporting Information. Cholesterol was purchased from Sigma-Aldrich. 2-(12-(7-Nitrobenz-2-oxa-1,3-diazol-4-yl)amino)dodecanoyl-1-hexadecanoyl-*sn*-glycero-3-phosphocholine (NBD-PC) was obtained from Molecular Probes (Leiden, The Netherlands). These lipids were dissolved in chloroform (HPLC grade) purchased from AppliChem (Darmstadt, Germany). The molecular structures for the lipids used here are shown in Figure 1.

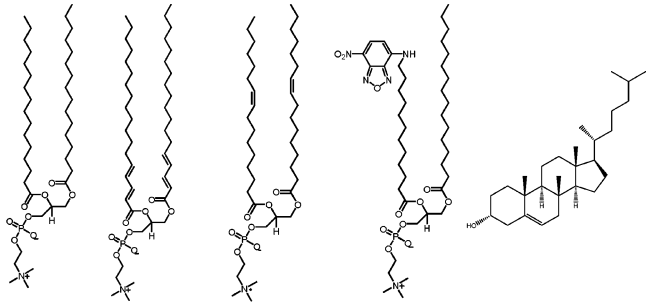

Figure 1. Molecular structures of lipids used in this study.

Stripe Pattern Formation. The mixed monolayers were obtained by spreading the lipid−chloroform solutions on the water surface (Millipore, resistance 18.2 MΩ·cm) using a microsyringe. Measurements of surface pressure−molecular area ($\pi-A$) isotherms were carried out using a computer-controlled commercial LB film balance system (NIMA 6100). The surface of the trough and the moving barrier are coated with Teflon. The temperature of the subphase was controlled by a thermostat (22.0 ± 0.3 °C), and the humidity of the laboratory was 50−70%. Following solvent evaporation for 15 min, the monolayers were symmetrically compressed at a constant speed of 10 cm^2/min. The monolayers at the mica surface were prepared as following. First, the freshly cleaved mica substrate (purchased from PLANO, Germany) was immersed into the pure water, and then the lipid−chloroform solution was spread on the subphase. After the monolayers were compressed to the predefined target pressure and stabilized for 30 min, they were deposited onto the mica surface by a vertical dipping method at a constant surface pressure and a constant dipping speed (1−60 mm/min).

Atomic Force Microscopy (AFM) Imaging. AFM images of the monolayers were acquired in air at room temperature with a commercial instrument (Digital Instruments, Nanoscope IIIa, Dimension 3000, Santa Barbara, CA) operating in tapping mode. Silicon cantilevers (Nanosensors) with spring constants 250−350 kHz were used. AFM images were flattened and are shown without any further image processing. The AFM images were analyzed by a self-developed program, written in the PW-Wave developing environment.[26]

Fluorescence Microscope. An epifluorescence microscope (Axioplan, Germany), equipped with a 63× long-distance objective (NA 0.90) and standard fluorescence filter sets, was used to record fluorescence images. Images were taken by a CCD camera (KAPPA, Germany), digitized by a frame-grabber card, and processed by imaging software.

Confocal Laser Scanning Microscope. Fluorescent images were acquired with a commercial confocal laser scanning microscope (Leica TCS SL, Heidelberg, Germany), equipped with a 63× oil immersion objective with a numerical aperture of 1.32 and Ar laser excitation.

Results and Discussion

Stripe Patterns Formed by Pure DPPC Monolayer. Previously, we obtained a periodic DPPC stripe pattern on mica at a surface pressure of ~3.0 mN/m (LE phase) with a high transfer velocity of 60 mm/min at ~22.5 °C.[12] The stripes (termed "horizontal stripes" here), as shown Figure 2a, are

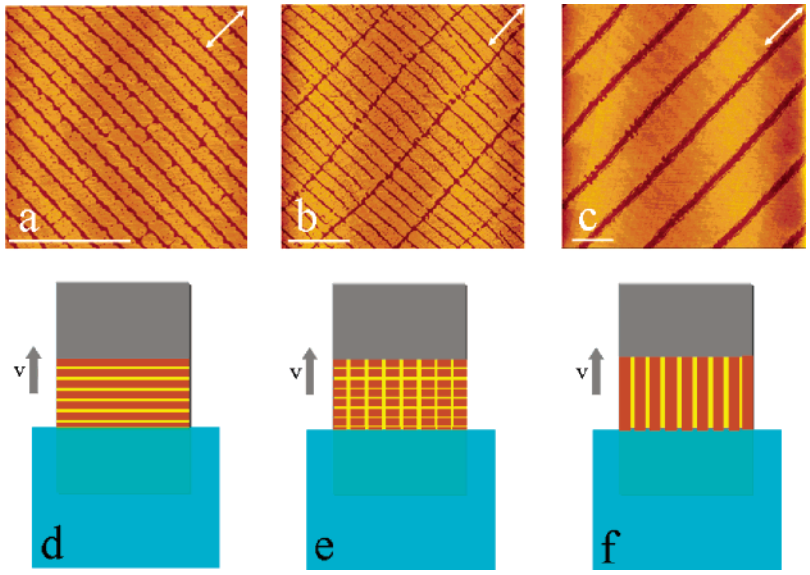

Figure 2. Stripe pattern formation by a pure DPPC monolayer. (a−c) Representative AFM images of the various pure DPPC patterns on mica surface that can be formed at various conditions below the main phase transition. Scale bar for these AFM images is 5 μm. Transfer conditions (transfer velocity and transfer surface pressure): (a) 60 mm/min and 3 mN/m, (b) 40 mm/min and 3 mN/m, and (c) 10 mm/min and 3 mN/m. Double arrow in the AFM images shows the axis of film transfer. (d−f) Schematic drawing illustrating the formation of various patterns during the LB vertical deposition.

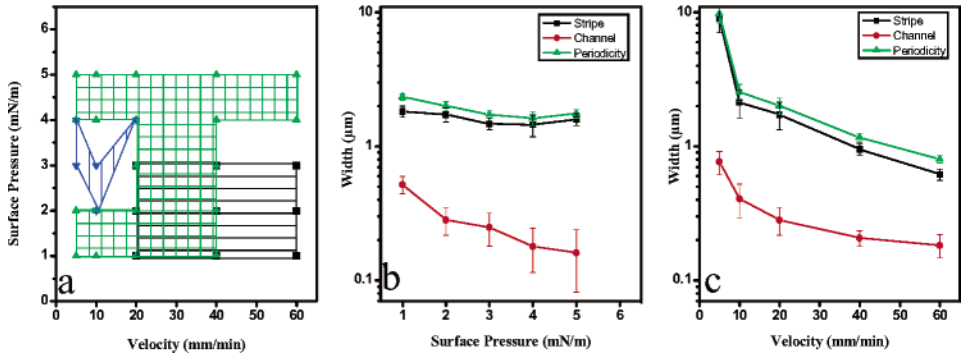

Figure 3. (a) Phase diagram of the stripe patterns on mica surface from a DPPC monolayer depending on transfer surface pressure and the transfer velocity depicted according to the results of AFM measurement. The phase diagram is composed of three different patterns: horizontal stripes (black ■), grid (green ▲), and vertical stripes (blue ▼). (b) Dependence of the widths of stripe and channel, and periodicity on the transfer surface pressure at a constant transfer velocity of 20 mm/min. (c) Dependence of the widths of the stripes, channels, and periodicity on the transfer velocity at a constant transfer surface pressure of 2 mN/m.

parallel to the three-phase contact line, i.e., perpendicular to the transfer direction. Although it is difficult to directly observe the stripe formation in situ at the three-phase contact line, one can imagine the process of stripe pattern formation as the schematic illustration of Figure 2d. When the substrate is pulled out, the DPPC molecules in LE phase at the contact line are pulled off from the water surface and transferred onto the substrate. The periodic stripe pattern formation was attributed to substrate-mediated condensation[9,11,12] of DPPC and meniscus oscillation[12] during LB vertical transfer. Moreover, we find that the transfer surface pressure and the transfer velocity play very important roles in the DPPC stripe pattern formation and a hypothesis involving the local curvature of the monolayer near the three-phase contact line was put forth.[17] At the same surface pressure (3 mN/m), vertical stripes, i.e., perpendicular to the three-phase contact line, as shown in Figure 2c, were observed at a low transfer velocity (10 mm/min). As shown in Figure 2f, the formation of a vertical stripe pattern appears to result from a fingering instability.[16,17] A similar vertical stripe pattern has been recently observed in lipid/lipopolymer mixed monolayer systems,[15] opening the possibility of extending LB patterning to other pattern-generating chemical systems. At the same surface pressure, when the transfer velocity is 40 mm/min, an intermediate pattern (termed "grid", as shown in Figure 2b) was observed, which clearly shows the superposition of horizontal stripes and vertical stripes. As the schematic drawing in Figure 2e shows, this kind of pattern might be induced by the coupling of the meniscus oscillation with a fingering instability.[16,17] Also, we find that on mica it is difficult to form pure horizontal stripes when the transfer velocity is less than 40 mm/min with pure DPPC molecules, and normally grid patterns mixed with horizontal stripe patterns are formed at the lower transfer velocity. Furthermore, by decreasing the transfer velocity, we can obtain much larger grids. According to the results of AFM measurements for different transfer conditions, we can depict a simplified phase diagram for the pure DPPC monolayer (Figure 3a) transferred onto a mica surface depending on the transfer surface pressure and velocity. For the pure DPPC, the horizontal stripes only appear at the high transfer velocity (40−60 mm/min) with low transfer surface pressure (black region in Figure 3a), while most of the cases are grid patterns (green region in Figure 3a). The superposition of black region and green region suggests that both horizontal stripe and grid patterns appear at the overlapped region. The vertical stripes only appear at the

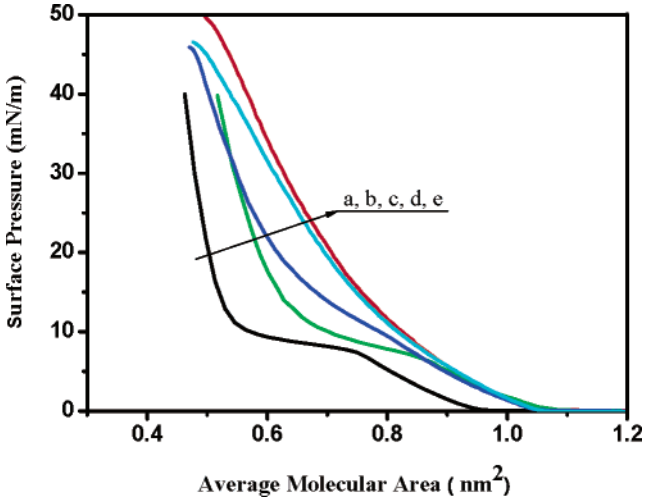

Figure 4. $\pi-A$ isotherms of DPPC/DOEPC mixed monolayers at the air−water interface depending on the molar fraction of DOEPC at 22.0 ± 0.3 °C. (a) DPPC, (b) DPPC/DOEPC (1:0.1), (c) DPPC/DOEPC (1:0.5), (d) DPPC/DOEPC (1:3), and (e) DOEPC.

low transfer velocity and high transfer surface pressure (blue region in Figure 3a).

Examination of stripe size (width and periodicity of the stripes) depending on the transfer surface pressure and velocity provides detailed information about the effect of transfer conditions on the pattern formation. Here, we focus on the size of the stripes perpendicular to the transfer direction. At the same transfer velocity (20 mm/min), increasing the transfer surface pressure from 1 to 5 mN/m decreases the width of the channels from 0.52 to 0.16 μm, but the stripe width and periodicity (stripe width + channel width) do not change much (Figure 3b). At the same transfer surface pressure (2 mN/m), increasing the transfer velocity from 5 to 60 mm/min decreases the widths of the channels and stripes from 0.77 to 0.18 μm and from 9.0 to 0.62 μm, respectively, and the mean periodicity from 9.8 to 0.80 μm, as shown in Figure 3c. The results here (on mica) look qualitatively similar to those for silicon.[17]

Stripe Patterns Formed by DPPC/DOEPC Mixed Monolayer. Figure 4 shows the $\pi-A$ isotherms of DPPC/DOEPC mixed monolayers of various compositions. In contrast to the pure DPPC monolayer, which has a horizontal region showing the typical LE−LC phase transition (curve a of Figure 4), the pure DOEPC monolayer takes a fully expanded phase (curve e of Figure 4) at the air−water interface before the monolayer collapses. This can be explained by the weak attractive intermolecular interaction of DOEPC, due to the kinks in the aliphatic chain of DOEPC owing to the presence of C=C bonds in the alkyl chains. The isotherms of mixed monolayers change systematically with the mixing ratio of the two components. When the molar fraction of DOEPC is below 33.3%, LE−LC phase transition remains. When the molar fraction of DOEPC is increased to above 75%, no shoulder-like region could be observed, which suggests no LE−LC phase transition at the air−water interface. Although DPPC and DOEPC show a low miscibility at high surface pressure (above the first-order phase transition point), i.e., DPPC in LC phase, and DOEPC in LE phase, they show high miscibility below the phase transition point (both in LE phase).

We did not obtain any domains when we transferred the pure DOEPC monolayer at the surface pressure below the collapsed pressure, which suggests that there is no substrate-mediated condensation for DOEPC at 22 °C. Furthermore, when we transferred the DPPC/DOEPC mixed monolayers below the phase transition point, i.e., a surface pressure corresponding to the LE state of DPPC and DOEPC, we observed some domains (stripes or dots, see further discussion) on mica by AFM measurement. Considering the properties of DOEPC, we can make sure that these domains are condensed DPPC which is formed due to the substrate-mediated condensation (also see further discussion).[11,12] Figure 5 shows the series of AFM images of DPPC/DOEPC (1:0.1) patterns on mica surface at the same transfer velocity (20 mm/min) with different transfer surface pressures. We then analyzed the size of stripes in detail in the same way as for pure DPPC patterns described above. At the same transfer velocity (20 mm/min), increasing the transfer surface pressure from 1 to 6 mN/m decreases the width of the channels from 0.73 to 0.13 μm, but the width and periodicity of the stripes show a minimum value at a surface pressure of about 3 mN/m (Figure 7b). In general, the width and periodicity of stripes in the mixed DPPC/DOEPC (1:0.1) patterns are ca. 4−6 times smaller than those of stripes formed by DPPC pure monolayer at the same transfer conditions. The width of channels, however, is similar. As described above, the transfer velocity is another important factor that can be used to tune the stripe patterns. Figure 6 shows the series of AFM images of DPPC/DOEPC (1:0.1) patterns on mica surface at the same transfer surface pressure (2 mN/m) with different transfer velocities. At high transfer velocity (60 mm/min), the stripes are not continuous, as shown in Figure 6a. However, when we decrease the transfer velocity below 40 mm/min, we can obtain continuous horizontal stripes. At the same transfer surface pressure (2 mN/m), decreasing the transfer velocity from 40 to 1 mm/min increases the widths of the channels and stripes from 0.30 to 2.1 μm and from 0.18 to 2.6 μm, respectively, and the mean periodicity from 0.48 to 4.8 μm, as shown in Figure 7c. Similar to the effect of surface pressure on the dimension of stripes, the width and periodicity of stripes in the mixed DPPC/DOEPC (1:0.1) patterns are about 4−5 times smaller than those of stripes in pure DPPC patterns at the same transfer conditions, while the width of channels is similar.

Similarly, we can obtain a phase diagram (Figure 7a) for the DPPC/DOEPC (1:0.1) monolayer patterns on mica surface according to the results of AFM measurements for different transfer conditions. It is surprising to see that most of the diagram in our experimental condition is covered by the black region (Figure 7a), which means horizontal stripe patterns. This would suggest that the ability to form horizontal stripes is increased after adding ~10 mol % DOEPC. At high transfer velocity (≥60 mm/min), there are no stripes or only broken stripes (red circles in Figure 7a). The grid pattern only appears at low transfer velocity (1 mm/min) and high transfer surface pressure (green triangles in Figure 7a). Compared with the phase diagram for the pure DPPC monolayer (Figure 3a), the phase diagram for the DPPC/DOEPC (1:0.1) mixed monolayer shifts to lower velocities and higher surface pressures. The question then is why the horizontal stripes dominate in the phase diagram for DPPC/DOEPC (1:0.1) mixed monolayer.

First of all, we address the question of where the DOPEC is, in the stripe or in the channel. We have identified that there is no substrate-mediated condensation of pure DOEPC under the experimental conditions used here. This would suggest that the DOEPC should still be in LE phase after the DPPC/DOEPC monolayer is transferred onto substrate. Then, we select NBD-PC as a molecular probe to detect its location with the help of fluorescence microcopy. It is well-known that NBD-PC would like to stay in the LE phase similar to DOEPC. If we can check the location of NBD-PC, then we will know the location of

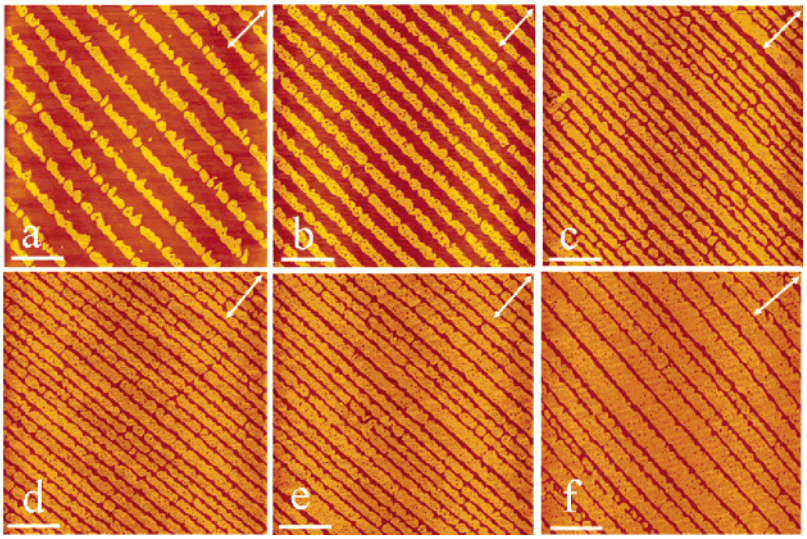

Figure 5. Tunable stripe pattern formation by the DPPC/DOEPC (1:0.1) mixed monolayer at transfer velocity of 20 mm/min with different surface pressures below the first-order phase transition. (a−f) Representative AFM images of DPPC/DOEPC (1:0.1) patterns on mica surface: (a) 1, (b) 2, (c) 3, (d) 4, (e) 5, and (f) 6 mN/m. Scale bar for these AFM images is 2 μm.

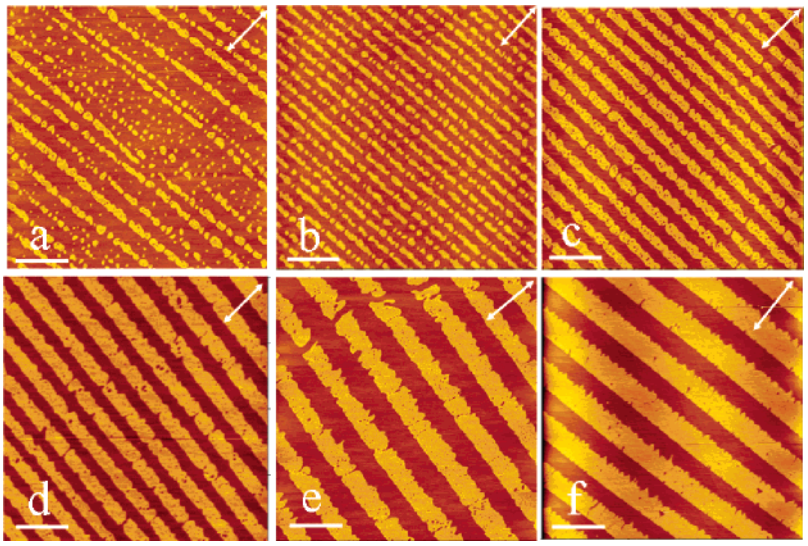

Figure 6. Tunable stripe patterns formation by the DPPC/DOEPC (1:0.1) mixed monolayer at surface pressure of 2 mN/m with different transfer velocities. (a−f) Representative AFM images of DPPC/DOEPC (1:0.1) patterns on mica surface: (a) 60, (b) 40, (c) 20, (d) 10, (e) 5, and (f) 1 mm/min. Scale bar for these AFM images is 2 μm.

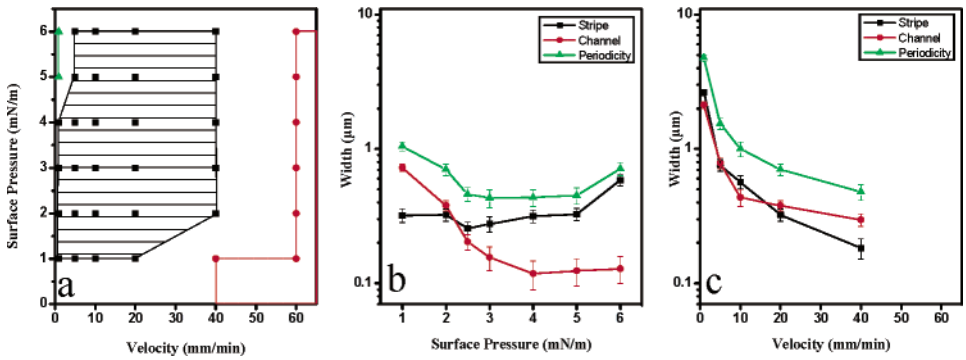

Figure 7. (a) Phase diagram of the stripe patterns on mica surface from the DPPC/DOEPC (1:0.1) mixed monolayer depending on transfer surface pressure and the transfer velocity depicted according to the results of AFM measurement. The phase diagram is composed of three different patterns: horizontal stripes (black ■), grid (green ▲), and no stripes or broken stripes (red ●). (b) Dependence of the widths of the stripes, channels, and periodicity on the transfer surface pressure at a constant transfer velocity of 20 mm/min. (c) Dependence of the widths of stripe and channel, and periodicity, on the transfer velocity at a constant transfer surface pressure of 2 mN/m.

DOEPC indirectly. Parts a and b of Figure 8 show the fluorescence microscopy image and confocal laser scanning microscopy image for the stripe patterns at mica surface from NBD-PC/DPPC (2 mol %) monolayer transferred at 3 mN/m and 40 mm/min. From these two images, it is clear that the green stripes are due to the fluorescence from NBD-PC.

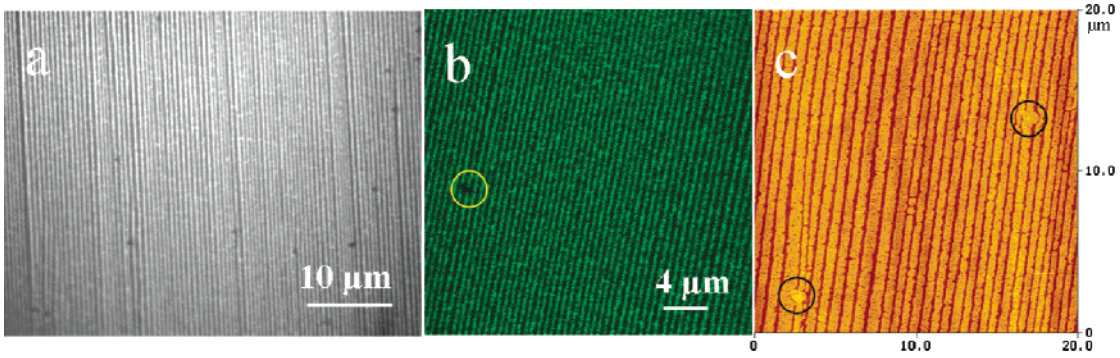

Figure 8. Stripe patterns on a mica surface from NBD-PC/DPPC (2 mol %) monolayer transferred at 3 mN/m and 40 mm/min. (a) Fluorescence microscopy image, (b) confocal laser scanning microscopy image, and (c) AFM image.

Furthermore, we observe some black circular domains in these two images. In AFM image (Figure 8c), we also observe some circular domains, which must be the condensed DPPC domains. Thus, we can make sure that the dark stripes in the fluorescence microscopy image and confocal laser scanning microscopy image are due to condensed DPPC stripes. Therefore, we make the conclusion that NBD-PC molecules stay in the channel. In a similar case, the observed stripe patterns from DPPC/DOEPC mixed monolayer can be apparently interpreted as a substrate-mediated microphase separation of liquid DOEPC and condensed DPPC during LB transfer. It is worth mentioning here that we used NBD-PC/DPPC stripes to check the stability of the sample. After 6 months stored in ambitious conditions in the lab, we did not observe essential changes either in the fluorescence microscopy image or in the AFM image.

The behavior of substrate-mediated condensation (or substrate-induced phase transition) during LB transfer is observed not only for phospholipid monolayers, such as DPPC[11,12] and L-α-dimyristoylphosphatidylethanolamine (DMPE),[32] but also for some fatty acid monolayers,[9,10] for instance tetradecanoic, pentadecanoic, and hexadecanoic acids. All of these monolayers at the temperature examined have the same property; i.e., the isotherms of the monolayers have a plateau region, representing the typical first-order phase transition of LE−LC. A simplified phase diagram would be useful to understand the phase transition at the air−water interface and the transition on the substrate during LB transfer. Dervichian[33] argued that there is a close connection between monolayer phases and the three-dimensional phases of the same substance. Therefore, according to the general phase diagram[34] and the phase diagram for long-chain acids,[35] we could simply depict a schematic phase diagram (Figure 9a) for DPPC monolayer at the air−water interface. Here, we use the solid phase to represent all of the condensed phases in order to simplify the discussion, although a multiplicity of condensed phases can be seen in the $\pi-T$ phase diagrams. As suggested by Knobler et al.,[36,37] the gas (G)−LE and LE−S transition lines merge at low temperatures, giving rise to the G−LE−S triple point, and below the triple point, a direct transition from a gas to a solid phase takes place. There is a general rule for the DPPC monolayer that the surface pressure of the LE−LC phase transition plateau will decrease with the decrease of the subphase temperature, so DPPC molecules tend to the LE−S phase transition if the system's temperature is decreased. Reconsidering the results of substrate-mediated DPPC condensation, we think that the LB transfer of DPPC monolayer in LE phase onto solid substrate is considered to be equivalent to decreasing the system's temperature, which induces the phase transition from liquid phase to solid phase, as the arrow shows in Figure 9a.

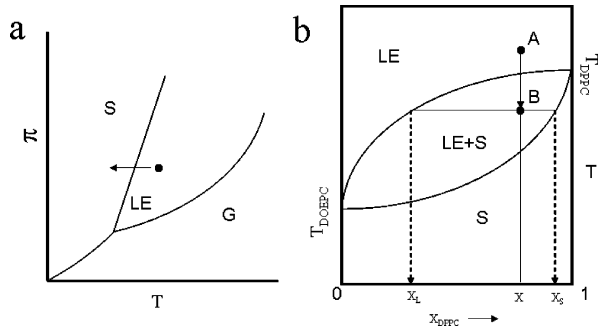

Figure 9. (a) Schematic phase diagram for DPPC monolayer. To simplify the discussion, this phase diagram omits the multiplicity of condensed phases. (b) Schematic phase diagram for DPPC/DOEPC mixed monolayer with full miscibility in the liquid state. The present phase diagram represents a case for the phase transition from LE phase to solid phase with the temperature decreasing.

Similarly, a simple phase diagram for DPPC/DOEPC mixed monolayer is graphically represented in Figure 9b, which is derived from the phase behavior of two lipids within a lipid bilayer membrane.[30] DPPC and DOEPC are homogeneously miscible in the liquid state (LE phase in the monolayer). DOEPC has a lower transition temperature (T_{DOEPC}) than DPPC (T_{DPPC}) does; thus the fluid phase and the solid phase coexist between the pure melting temperatures of both lipids (namely, between T_{DOEPC} and T_{DPPC}). We consider only the phase transition from the LE phase to the solid phase with the temperature decreasing. Starting with a DPPC/DOEPC (1:0.1) mixture in the LE phase (point A in Figure 9b), LB transfer from LE monolayer phase implies the decrease of temperature; thus the phase is shifted from point A to point B. According to the phase diagram, the fluid phase is enriched by the lower melting lipid (DOEPC), while the solid phase is enriched with the higher melting lipid (DPPC). At point B, there is a microphase separation of DOEPC and DPPC, which makes the switch between substrate-mediated condensed-phase transfer and liquid-phase transfer[26] become faster. The amplitude of this switch should determine the width and periodicity of stripes; thus we can understand why the width and periodicity of stripes in the mixed DPPC/DOEPC (1:0.1) patterns are smaller than those in pure DPPC patterns at the same transfer conditions. From the above discussion, we can also conclude that the addition of DOEPC into the DPPC monolayer decreases the extent of substrate-mediated condensation of DPPC compared with that of the pure DPPC monolayer. Normally, for a pure DPPC monolayer, the fingering instability to form vertical stripes happens at lower transfer velocities and high surface density of DPPC molecule in LE phase (Figure 3a). Therefore, in the case of DPPC/DOEPC mixed monolayer, the conditions to form vertical stripes should be much lower

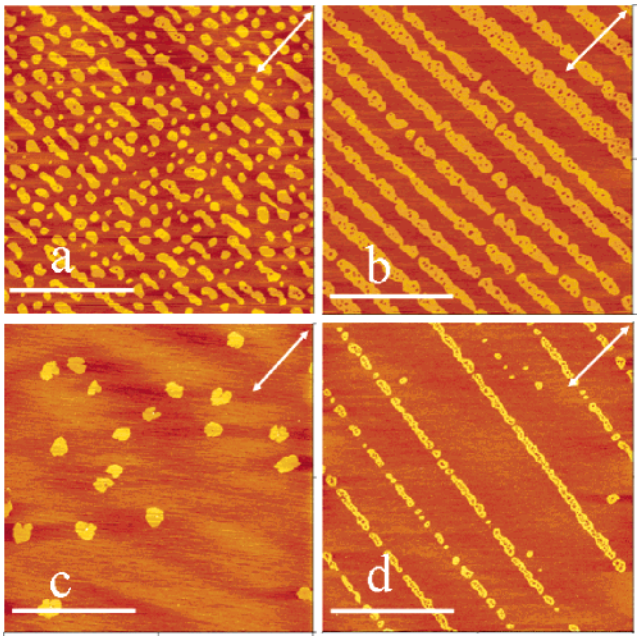

Figure 10. Patterns formed by DPPC/DOEPC (1:0.5) monolayer at surface pressure of 8 mN/m with different transfer velocities: (a) 10 and (b) 5 mm/min. Patterns formed by DPPC/DOEPC (1:3) monolayers at surface pressure of 20 mN/m with different transfer velocities: (c) 10 and (d) 5 mm/min. Scale bar for these AFM images is 2 μm.

velocity or higher surface pressure, which is confirmed by our experiment (Figure 7a; we only obtain grid patterns at the transfer velocity of 1 mm/min and the transfer surface pressure of 5−6 mN/m). Therefore, for DPPC/DOEPC (1:0.1) mixed monolayer, the extent of substrate-mediated condensation of DPPC is decreased with addition of DOEPC, which is the reason for the shift of the phase diagram and the domination of horizontal stripes in the phase diagram.

We also find that the molar fraction of DOPEPC in DPPC/DOEPC mixed monolayers plays an important role in the formation of horizontal stripes. If we increase the molar fraction of DOEPC to 33.3%, the critical transfer velocity to form the horizontal stripe pattern is about 5 mm/min at the surface pressure of 8 mN/m (Figure 10b), which is much different from the case of DPPC/DOEPC (1:0.1) (2 mN/m and 40 mm/min). There are broken stripes when the transfer velocity is larger than 5 mm/min, as shown in Figure 10a. Further increasing the molar fraction of DOEPC decreases the ability to form stripe patterns. For instance, when the molar fraction of DOEPC is increased to 75%, even at the surface pressure of 20 mN/m there are only disordered circular domains (Figure 10c) or broken stripes (Figure 10d). Considering all of these results, we can conclude that, at the same transfer conditions, the ability to form stripe patterns (or the ability of substrate-mediated condensation) is decreased if the molar fraction of DOEPC is increased.

Effect of Other Lipids. Meanwhile, we note that not only DOEPC, but also other lipids, such as DPOPC and cholesterol, can affect the DPPC stripe formation. For instance, at a transfer surface pressure of 2 mN/m and a transfer velocity of 20 mm/min, for a DPOPC/DPPC (2 mol %) mixed monolayer (Figure 11a), the mean periodicity of stripes is about 0.8 μm, which is smaller than that (~2 μm) of the pure DPPC monolayers. Contrary to DPOPC, which has a structure similar to that of DPPC, cholesterol has a structure completely different from that of DPPC. However, cholesterol has a similar effect on stripe formation. For cholesterol/DPPC (2 mol %) monolayer, at a transfer surface pressure of 2 mN/m and a transfer velocity of

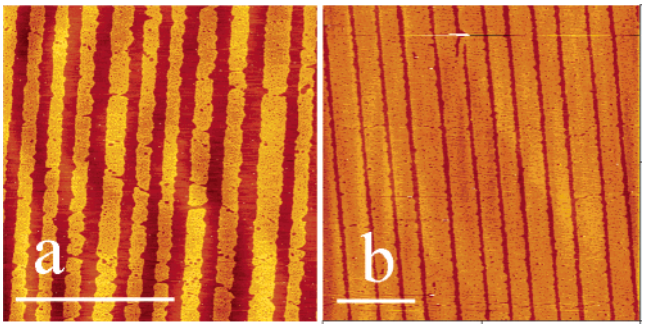

Figure 11. Stripe patterns formed from (a) DPOPC/DPPC (2 mol %) monolayer, and (b) cholesterol/DPPC (2 mol %) monolayer at the same transfer conditions (2 mN/m, 20 mm/min). Scale bar for these AFM images is 5 μm.

20 mm/min, the mean periodicity of stripe is 1.4 μm (Figure 11b), which also is smaller that (~2 μm) from pure DPPC monolayer. It is clear that the extent of the effect on the stripe formation is different for DPOPC and cholesterol, which could be due to the different miscibility and diffusion coefficients of the lipid in the monolayer. Thus, during the LB transfer, different lipids affect the extent of substrate-mediated condensation of DPPC differently.

Conclusions

In summary, we have systematically investigated the effect of a second component on the formation of DPPC microstripe patterns by the LB technique. Generally, the width and periodicity of the stripes formed from mixed monolayer are smaller than those of stripes formed from pure DPPC patterns at the same transfer conditions. The reason is that upon addition of the second component the extent of substrate-mediated condensation of DPPC during LB transfer is decreased. The microphase separation of DPPC during the LB transfer can be influenced by adding the second lipid component, which makes the tuning of stripe patterns more effective. The ability to tune stripe patterns by adding the second component in DPPC monolayer will increase the versatility of LB patterning for surface pattern engineering.

Acknowledgment. Dr. S. Lenhert is acknowledged for his helpful discussion and critically reading the manuscript. This work was supported by the Deutsche Forschungsgemeinschaft as a contribution from the SFB 424, the China National Natural Science Foundation (20373019), and the China−Germany Collaboration Project (50520130316). L.W. wishes to thank the Deutsche Forschungsgemeinschaft for support as a visiting scholar.

Supporting Information Available: Details of the synthesis of DOEPC. This material is available free of charge via the Internet at http://pubs.acs.org.

References and Notes

(1) Whitesides, G. M.; Love, J. C. *Sci. Am.* **2001**, *285* (3), 38−47.
(2) Park, M.; Harrison, C.; Chaikin, P. M.; Register, R. A.; Adamson, D. H. *Science* **1997**, *276*, 1401−1404.
(3) Haynes, C. L.; Van Duyne, R. P. *J. Phys. Chem. B* **2001**, *105*, 5599−5611.
(4) Mcconnell, H. M. *Annu. Rev. Phys. Chem.* **1991**, *42*, 171−195.
(5) Mohwald, H. *Annu. Rev. Phys. Chem.* **1990**, *41*, 441−476.
(6) Nandi, N.; Vollhardt, D. *Chem. Rev.* **2003**, *103*, 4033−4075.
(7) Legrange, J. D. *Phys. Rev. Lett.* **1991**, *66*, 37−40.
(8) Riegler, J. E.; Legrange, J. D. *Phys. Rev. Lett.* **1988**, *61*, 2492−2495.

(9) Sikes, H. D.; Woodward, J. T.; Schwartz, D. K. *J. Phys. Chem.* **1996**, *100*, 9093−9097.
(10) Sikes, H. D.; Schwartz, D. K. *Langmuir* **1997**, *13*, 4704−4709.
(11) Spratte, K.; Chi, L. F.; Riegler, H. *Europhys. Lett.* **1994**, *25*, 211−217.
(12) Gleiche, M.; Chi, L. F.; Fuchs, H. *Nature* **2000**, *403*, 173−175.
(13) Moraille, P.; Badia, A. *Langmuir* **2002**, *18*, 4414−4419.
(14) Moraille, P.; Badia, A. *Langmuir* **2003**, *19*, 8041−8049.
(15) Purrucker, O.; Fortig, A.; Ludtke, K.; Jordan, R.; Tanaka, M. *J. Am. Chem. Soc.* **2005**, *127*, 1258−1264.
(16) Lenhert, S.; Zhang, L.; Mueller, J.; Wiesmann, H. P.; Erker, G.; Fuchs, H.; Chi, L. F. *Adv. Mater.* **2004**, *16*, 619−624.
(17) Lenhert, S.; Gleiche, M.; Fuchs, H.; Chi, L. F. *ChemPhysChem* **2005**, *6*, 2495−2498.
(18) Mahnke, J.; Vollhardt, D.; Stockelhuber, K. W.; Meine, K.; Schulze, H. J. *Langmuir* **1999**, *15*, 8220−8224.
(19) Kovalchuk, V. I.; Bondarenko, M. P.; Zholkovskiy, E. K.; Vollhardt, A. *J. Phys. Chem. B* **2003**, *107*, 3486−3495.
(20) Gleiche, M.; Chi, L. F.; Gedig, E.; Fuchs, H. *ChemPhysChem* **2001**, *2*, 187−191.
(21) Lu, N.; Chen, X. D.; Molenda, D.; Naber, A.; Fuchs, H.; Talapin, D. V.; Weller, H.; Muller, J.; Lupton, J. M.; Feldmann, J.; Rogach, A. L.; Chi, L. F. *Nano Lett.* **2004**, *4*, 885−888.
(22) Moraille, P.; Badia, A. *Angew. Chem., Int. Ed.* **2002**, *41*, 4303−4306.
(23) Lu, N.; Gleiche, M.; Zheng, J. W.; Lenhert, S.; Xu, B.; Chi, L. F.; Fuchs, H. *Adv. Mater.* **2002**, *14*, 1812−1815.
(24) Zhang, M. Z.; Lenhert, S.; Wang, M.; Chi, L. F.; Lu, N.; Fuchs, H.; Ming, N. B. *Adv. Mater.* **2004**, *16*, 409−413.
(25) Lenhert, S.; Meier, M. B.; Meyer, U.; Chi, L. F.; Wiesmann, H. P. *Biomaterials* **2005**, *26*, 563−570.
(26) Chen, X. D.; Hirtz, M.; Fuchs, H.; Chi, L. F. *Adv. Mater.* **2005**, *17*, 2881−2885.
(27) Gains, L. G. *Insoluble Monolayers at Liquid−Gas Interfaces*; Interscience Publishers: New York, 1969.
(28) Discher, B. M.; Schief, W. R.; Vogel, V.; Hall, S. B. *Biophys. J.* **1999**, *77*, 2051−2061.
(29) Discher, B. M.; Maloney, K. M.; Schief, W. R.; Grainger, D. W.; Vogel, V.; Hall, S. B. *Biophys. J.* **1996**, *71*, 2583−2590.
(30) Binder, W. H.; Barragan, V.; Menger, F. M. *Angew. Chem., Int. Ed.* **2003**, *42*, 5802−5827.
(31) Dorn, K.; Klingbiel, R. T.; Specht, D. P.; Tyminski, P. N.; Ringsdorf, H.; Obrien, D. F. *J. Am. Chem. Soc.* **1984**, *106*, 1627−1633.
(32) Gleiche, M. Procedure for the production of periodic structures by wetting instabilities. Ph.D. Thesis, University of Muenster, Muenster, Germany, 2001.
(33) Dervichian, D. G. *J. Chem. Phys.* **1939**, *7*, 931−948.
(34) Atkins, P.; de Paula, J. *Atkins' Physical Chemistry*; Oxford University Press: New York, 2002; pp 135−150.
(35) Knobler, C. M.; Desai, R. C. *Annu. Rev. Phys. Chem.* **1992**, *43*, 207−236.
(36) Knobler, C. M. *Science* **1990**, *249*, 870−874.
(37) Moore, B. G.; Knobler, C. M.; Akamatsu, S.; Rondelez, F. *J. Phys. Chem.* **1990**, *94*, 4588−4595.